Published in final edited form as:
J Bone Miner Res. 2014 March ; 29(3): 705–715. doi:10.1002/jbmr.2064.

Deletion of a Single β-catenin Allele in Osteocytes Abolishes the Bone Anabolic Response to Loading

B. Javaheri[1], **A. Stern**[2,3,4], **N. Lara**[2], **M. Dallas**[2], **H Zhao**[2], **Y Liu**[2], **L.F. Bonewald**[2], and **M.L. Johnson**[2]

[2]UMKC School of Dentistry, Department of Oral and Craniofacial Sciences, Kansas City, MO 64108

[3]UMKC School of Computing and Engineering, Department of Civil and Mechanical Engineering, Kansas City, MO 64110

[4]Engineering Systems Incorporated, 8541 Crown Crescent CT., Charlotte, NC. 28227

Abstract

The Wnt/β-catenin signaling pathway is essential for bone cell viability, function and for skeletal integrity. To determine if β-catenin in osteocytes plays a role in the bone anabolic response to mechanical loading, 18-24 wk old osteocyte β-catenin haploinsufficient mice (Dmp1-Cre x β-catenin fl/+; HET cKO) were compared to their β-catenin fl/fl (control) littermates. Trabecular BV/TV was significantly less (58.3%) in HET cKO females versus controls, while male HET cKO and control mice were not significantly different. Trabecular number was significantly less in HET cKO mice compared to controls for both genders and trabecular separation was greater in female HET cKO mice. Osteoclast surface was significantly greater in female HET cKO mice. Cortical bone parameters in males and females showed subtle or no differences between HET cKO and controls. The right ulnae were loaded *in vivo* at 100 cycles, 2 Hz, 2500 με, 3 days per week for 3 weeks and the left ulnae served as non-loaded controls. Calcein and alizarin complexone dihydrate were injected 10 days and 3 days prior to sacrifice, respectively. MicroCT analysis detected an 8.7% and 7.1% increase in cortical thickness in the loaded right ulnae of male and female control mice, respectively, compared to their non-loaded left ulnae. No significant increase in new cortical bone formation was observed in the HET cKO mice. Histomorphometric analysis of control mice showed a significant increase in endocortical and periosteal mineral apposition rate (MAR), BFR/BS, BFR/BV and BFR/TV in response to loading, but no significant increases were detected in the loaded HET cKO mice. These data show that deleting a single copy of β-catenin in osteocytes abolishes the anabolic response to loading and that trabecular bone in females is more severely affected and suggest that a critical threshold of β-catenin is required for bone formation in response to mechanical loading.

Send all Correspondence to Mark L. Johnson, Ph.D. Professor and Chair Department of Oral and Craniofacial Sciences UMKC School of Dentistry 650 East 25th street Kansas City, MO 64108.
[1]Current address: The Royal Veterinary College, Royal College Street, London, NW1 0TU, United Kingdom

Disclosure Statement: All authors state that they have no conflicts of interest.

Keywords

β-catenin; Mechanical Loading; Osteocyte; Bone Formation

Introduction

Bone adapts its mass and architecture in response to mechanical loading, but the exact cellular mechanisms that mediate this adaptive response are not fully understood. Studies of human mutations that result in altered bone mass phenotypes first suggested an important role for the Wnt/β-catenin signaling pathway in bone mass accrual [1–3] and the possible role of this pathway in bone response to mechanical loading [4]. There is now clear evidence that Wnt/β-catenin signaling is one of the pathways that is activated and involved in bone cells response to mechanical load [5–15]. We have proposed a model in which osteocytes initially activate β-catenin signaling in response to mechanical loading in part through an Akt dependent – Lrp5/6 independent mechanism [16]. *In vitro* evidence using osteoblastic and osteocytic cells supports this model [13,14,17].

The Wnt/β-catenin signaling pathway also regulates basal bone mass through a number of different mechanisms including renewal of stem cells [18], stimulation of osteoblast differentiation and proliferation [19], enhancement of osteoblast activity [19,20] and inhibition of osteoblast and osteocyte apoptosis [21]. Conditional deletion of β-catenin in osteoblasts *in vivo* using alpha 1 type I collagen Cre [22] or osteocalcin-Cre [23] showed that osteoblast regulation of osteoclast differentiation was dependent on Wnt/β-catenin signaling. The mechanism underlying the fragile bone phenotype in these mice is apparently due to increased osteoclastic bone resorption as a result of decreased expression of osteoprotegerin[22,23]. Interestingly, mice with targeted deletion in osteocytes are born normal but display progressive bone loss with age accompanied by growth retardation and premature lethality [24]. Cancellous bone mass is almost completely lost and cortical bone thickness is severely reduced. The low bone mass correlates with increased osteoclast number and activity due to an increased osteocyte RANKL/OPG ratio [24]. Given that the osteocyte is now recognized as an important source of RANKL [25–27] in bone this raises the intriguing question of how much of the observed phenotype in the osteoblast targeted deletions of β-catenin might have been due to osteocyte loss of β-catenin signaling in those mice [22,23].

The osteocyte is widely believed to be the main mechanosensory cell in bone [16], but there is limited *in vivo* evidence demonstrating a clear role for the β-catenin signaling pathway in osteocytes with regards to anabolic loading induced bone formation. The targeted homozygous deletion of β-catenin in osteocytes results in a severely fragile skeleton and these mice do not live much beyond 8 weeks of age [24] making it impossible to perform *in vivo* mechanical loading studies with these mice. However, the skeletal phenotype of the heterozygous mice with the loss of a single β-catenin allele is relatively normal at 2 months of age with the exception that cancellous bone volume is decreased by about 10% in heterozygous male and about 25% in heterozygous female mice relative to control littermates [24].

Therefore in order to determine whether β-catenin is required for the anabolic bone formation response to mechanical loading, we conditionally deleted a single allele of β-catenin in osteocytes (designated HET cKO) by crossing β-catenin fl/fl (designated control) mice with Dmp1-Cre mice. We report our findings on the characterization of the adult skeleton and response to anabolic loading of these heterozygous mice and their fl/fl control littermates at 18-24 weeks of age. Our loading studies demonstrate that deletion of a single allele of β-catenin in osteocytes abolishes anabolic load-induced new bone formation. Our studies also revealed major gender differences in trabecular bone phenotypes in HET cKO mice with a more severe effect of osteocyte β-catenin haploinsufficiency observed in females.

Methods

Mouse lines and breeding

The β–catenin fl/fl (exon 2–6) mice (control) were purchased originally from Jackson Laboratories (B6.129-Catnb^{tm2Kem}/J; Jackson Laboratories, Bar Harbor, ME). The β–catenin fl/fl mice were crossed with the 10Kb Dmp1-Cre mice [(28)] to produce mice with a heterozygous deletion of β-catenin in osteocytes. All mice were 18-24 weeks old. The studies described in this manuscript were approved by the UMKC Institutional Animal Care and Use Committee.

TRAP Staining

Femurs from male (n=3) and female (n=3) β-catenin fl/fl (control) and HET cKO (male n=3 and female n=5) were excised, cleaned of soft tissue, placed in ice-cold 4% paraformaldehyde for 24 hours, and decalcified in EDTA for one week. Paraffin-embedded histological sections were stained for TRAP. TRAP positive osteoclasts were quantified using the OsteoMeasure Histomorphometry System (Osteometrics Inc., Decatur, GA) in a standard zone of 1 mm starting 200 μm below the growth plate (to exclude primary spongiosa) and 100 μm from the cortical bone (to avoid trabecular area associated with cortical bone). Osteoclast numbers were expressed as N.Oc/BPm and Oc.S/BS according to accepted histomorphometric standards [(29)].

High-resolution microcomputed tomography (μCT)

MicroCT analysis of femur/tibia (n=7 for male and female controls and male HET cKO mice; n=9 for female HET cKO) for baseline characterization and right/left ulnae for loading studies (n=6 for male and female controls and n=5 for male and female HET cKO) was conducted using a Scanco *viva*CT40 (Scanco Inc., Basel, Switzerland) at a resolution of 10 μm for femurs and tibia and 15 μm for ulna, 55kV voltage, 145 μA current and 200 ms integration time following recommended guidelines [(30)]. Analysis was performed on post mortem femurs/tibias that were fixed in 70% ethanol or once embedded in plastic in the case of the ulnae. Using our standard approach for adult bones, a high resolution scan of the region of interest was performed. For ulna, the 1 mm between the 2–3 mm distal to midshaft was analyzed. The threshold used for trabecular and cortical bone was set to 300 and 350 respectively. The region of analysis is shown in figure 1 and comprised 30 slices of secondary spongiosa beginning just beneath the region of primary spongiosa. Three

dimensional images were generated using the following values: gauss filter: σ= 0.8; support = 1; and threshold as noted above. Three dimensional analyses were performed to determine bone volume/tissue volume, trabecular number, trabecular thickness, and trabecular separation at the proximal femur and distal tibia. Cortical bone was measured at the mid-shaft region of the bone. Quantitation of BMD of the bone samples was determined by comparison against a hydroxyapatite standard (Scanco Inc.) that was scanned weekly for instrument calibration.

Strain gaging and in vivo loading

For *ex vivo* strain gaging analysis the gages were applied to the ulnae at 2 mm distal to the ulna mid-shaft on the medial surface and at a site 5 mm distal to the end of the olecranon process on the lateral surface. Uniaxial strain gages (EA-06-015DJ-120 -option, Vishay Micro-Measurements; Raleigh, NC) were glued (Bond 200 kit, Measurements Group) to the lateral surface and parallel to the longitudinal axis. The forearms (n=3 per gender and genotype) were placed in the loading system (EnduraTEC ELF 3200 Loading device, BOSE Corp., Minnetonka, MN) and the device cycled at least 4 times to ascertain that a stable waveform was obtained before starting data collection. Strain measurements were made using an electronic bridge conditioner Model 7000-32-SM (Vishay Micro-Measurements; Raleigh, NC) and digitally displayed using StrainSmart software (Vishay Micro-Measurements; Raleigh, NC). After application of strain gages, loading was conducted on the right forearm at 2 Hz, using a haversine waveform for 15 cycles. Loading was conducted at −0.5, −1, −1.5, −2, −2.5, −3 and −3.5N for the intact forearm. Strains in the last five cycles were averaged.

In vivo loading was performed on the right ulna of each mouse under compression using the EnduraTEC ELF 3200 Loading device (BOSE Corp., Minnetonka, MN). Each loading session was conducted for 100 cycles at 2 Hz. The magnitude of load applied was 2.25N, sufficient to produce a global strain of 2500 με [(10)]. The left ulnae serve as a contralateral non-loaded control. Loading was performed three days per week (MWF) for three weeks.

Bone formation analysis

During the 3 week loading regimen, mice were injected with calcein (5 mg/kg) and alizarin red (20 mg/kg) (Sigma Chemical Company, St. Louis, MO) 10 and 3 days (respectively) prior to sacrifice and collection of bone samples. The forearms were dissected, fixed in 4% paraformaldehyde (Alfa Aesar Inc. Ward Hill, MA), methyl methacrylate embedded and sectioned at a thickness of 20 μm. Sections were taken from the blocks containing bone 3 mm distal to midshaft. Standard bone histomorphometry was performed using the OsteoMeasure Histomorphometry System. This software follows ASBMR nomenclature for bone histomorphometry[(29)]. Mineral apposition rate (MAR) and bone formation rate (BFR) on the endocortical (Ec) and periosteal (Ps) surfaces were calculated from comparable sections obtained in the midshaft region of the loaded and non-loaded ulnae. BFR was normalized against either the bone surface (BS), bone volume (BV) or the tissue volume (TV) as determined by the software per standard convention[(29)]. Periosteal (Ps) and endocortical (Ec) single label (sL) surfaces (S) were also determined as a function of total bone surface.

Ash content

The right and left femurs were processed to determine final mineral content by measurement of ash fraction [31]. Dry mass was obtained by drying in oven at 100°C for 24 hours followed by 600°C for 24 hours in a muffle furnace. Ash weight was measured and ash content was expressed as percentage of dry ash mass/dry mass.

Three-point bending to failure

Displacement controlled three-point bending to failure tests were conducted on tibiae and femurs *ex vivo* to characterize the biomechanical properties of the bones. Tibiae and femurs were harvested from freshly sacrificed mice. The associated soft tissue was removed and the bones were individually wrapped in saline soaked gauze and stored at −20°C until testing. Prior to biomechanical testing, samples were allowed to thaw and reach room temperature. Samples were kept hydrated with saline soaked gauze and not allowed to dry out prior to, or during testing. Span lengths of 7.6 mm were used for the samples and the bones were placed into the fixture so they would be impacted in what would be the anterior to posterior direction *in vivo*. A crosshead displacement rate of 0.1 mm/s was used. Crosshead displacement and axial load were recorded at a rate of 70 Hz. The stiffness and ultimate force were calculated from the resulting load verses displacement curves for each bone. The Young's Modulus (*E*) for each bone was calculated using the following equation:

$$E=\frac{Sl^3}{48I}$$

where; *S* is the stiffness, *l* is the span length, and *I* is the area moment of inertia. The area moment of inertia was calculated across the mid-span at the fracture location using ten slices mid-span of the realigned μCT scans using the BoneJ plug-in for the image processing program ImageJ (BoneJ, NIH, USA) [32,33].

Statistical Analysis

Two-way ANOVA (analysis of variance) was used to investigate the effect of gender and treatment. A least square t-test was applied to identify significant differences between control and HET cKO within the same gender and to test for significance between female and male within each treatment level. A repeated measurements test was utilized to investigate the effect of treatment (parameter measured) and loading and gender in which loading was designated as the within-subject variable with two levels (load and non-load) and two between-subject variables: gender and treatment. If a significant interaction was detected, then a simple effect test was applied to identify the significant treatment effect within same experimental condition. Data analysis was performed with SPSS (Statistical Package for Social Science, version 20; SPSS Inc., Chicago, IL). A $p<0.05$ was considered significant.

Results

Basal bone properties of HET cKO mice

Homozygous deletion of β-catenin in osteocytes results in a skeleton that is too frail to withstand *in vivo* forearm loading [24]. We therefore used a heterozygous deletion of β–catenin strategy in which β-catenin fl/fl mice were crossed with the 10kb Dmp1-Cre mice, which results in the loss of one allele of β-catenin principally in osteocytes (HET cKO). These mice are long lived and able to undergo forearm compression loading without evidence of fracture. MicroCT analysis revealed no significant differences (ns) in femoral trabecular bone mineral density (BMD) (Figure 1B) or cortical BMD (Figure 1H), although percentage ash content was lower in the HET cKO mice compared to their gender controls ($p<0.05$). 3D images (Figure 1A) show decreased trabecular content in female HET cKO mice and quantitative analysis demonstrated that femoral trabecular BV/TV was 58.3% less ($p<0.05$) in HET cKO females and 19.1% less (not significant, ns) in HET cKO males as compared to male controls (Figure 1C). Both control and HET cKO females showed lower BV/TV ($p<0.05$) compared to their male counterparts (Figure 1C). Significant decreases in trabecular number were observed in both genders with females significantly lower than their male counterparts (Figure 1D). Trabecular separation was significantly ($p<0.05$) increased in females versus males and in female HET cKO versus female controls (Figure 1F). Female HET cKO mice also had significantly decreased ($p<0.05$) trabecular thickness compared to male HET cKO. Female cortical HET cKO BV/TV was significantly lower compared to female control mice, but cortical thickness was not different (Figure 1I–1J). Similar findings were observed in the microCT analysis of the proximal tibia (Supplemental Figure 1).

Histological analysis (Figure 2) revealed a significant increase in the number of TRAP positive osteoclasts in female HET cKO compared to male HET cKO and to female control ($p<0.05$) (Figure 2B). Osteoclast surface per total bone surface in female HET cKO was significantly higher compared to female control and male HET cKO ($p<0.05$) (Figure 2C).

Biomechanical properties of osteocyte β–catenin HET cKO mice

We next characterized the biomechanical properties of the femurs and tibiae from these mice using *ex vivo* three-point bending to failure. The stiffness, ultimate force, and Young's modulus were determined. There were no significant differences found between the control and the HET cKO mice for the femurs and tibiae isolated from either males or females (Figure 3 and Supplemental Figure 2). We observed a statistically significant increase in the femoral Young's Modulus (Figure 3) in the female mice compared to their male counterparts ($p<0.05$), but no difference in the HET cKO mice of either gender compared to their gender controls. Tibial mechanical properties showed reduced ultimate load in female mice compared to their male counterparts.

In vivo bone formation response to loading

Prior to mechanical loading, the strain:load relationship of the ulnae from HET cKO and control mice was determined using strain gage measurements. As shown in Figure 4 there were no statistically significant differences in the strain:load curves between males and females and/or between HET cKO compared to control ulnae. A load of 2.25 N was applied

to the right forearms of all mice producing a global strain level of ~2500 με. As expected, there was a significant increase in new bone formation in the control groups in the loaded compared to the non-loaded ulnae for both males and females on both the periosteal and endocortical surfaces as shown by double fluorochrome labeling (Figure 5 and 6). However, the load response observed in the control mice was not observed in the HET cKO group (both female and male) as evidenced by little or no double labeling (Figure 5 and 6). The HET cKO mice also had significantly lower amounts of single label surfaces compared to their controls for both loaded and non-loaded groups of male and female mice (Table 1). Quantitation of the mineral apposition rates (MAR) and bone formation rate (BFR) using histomorphometric analysis indicated a statistically significant increase in the MAR and normalized BFRs, comparing the loaded versus the non-loaded ulnae of the control group (Figure 6A and 6B and Table 1). In contrast to controls, male and female HET cKO loaded ulnae MAR and BFRs on both the endocortical and periosteal surfaces were not significantly different from the non-loaded ulnae (Figure 6A and 6B and Table 1). MicroCT analysis of loaded and non-loaded ulnae obtained at the end of the 3 week loading regimen also demonstrated significant increases in control mice cortical thickness (8.7% in males and 7.1% in females) at the midshaft of the ulna corresponding to the region assessed by dynamic histomorphometry (Figure 6C and Supplemental Figure 3).

Discussion

The Wnt/β-catenin signaling pathway plays an important role in bone mass regulation. In addition, the osteocytes play an important role in the regulation of osteoblasts and osteoclasts activity and their role in mechanosensation and responsiveness in bone [16]. Previous work by Kramer *et al*[24] demonstrated that homozygous deletion of β-catenin targeted to osteocytes resulted in a severely compromised skeleton by 5–8 weeks of age, whereas the deletion of a single allele had little or no effect at this young age. Therefore, to better understand the role of β-catenin in the adult skeleton we examined the basal bone phenotypes and new bone formation response to anabolic loading in male and female mice, lacking a single allele of β-catenin in osteocytes.

Characterization of the basal bone phenotype revealed major gender differences as a result of the targeted deletion of a single allele of β-catenin in osteocytes in trabecular bone of female compared to male mice, yet no differences in cortical bone. We performed microCT measurements on 30 slices proximal to the primary spongiosa of the distal femur and immediately distal to the primary spongiosa of the proximal tibia. Trabecular BV/TV was significantly reduced in female mice by 58.3% ($p<0.05$), while trabecular BV/TV in male mice was decreased 19.1% but was not statistically significant from controls ($p=0.745$). However the 3D images suggest that there is less trabecular content in the male HET cKO towards the femur midshaft, but is still less evident compared to female mice. The data from Kramer *et al*., [24] indicated a ~25% reduction in cancellous bone volume in female mice and a non-significant reduction in male mice at 8 weeks of age. Thus, our data indicates that the trabecular bone phenotype of the HET cKO mice continues to progressively worsen with aging. The decrease in trabecular BV/TV appears to be due to increased osteoclast activity as observed by histological analysis, supporting the concept that β-catenin in osteocytes regulates osteoclastogenesis [25–27]. Given that RANKL expression in the osteocyte is also

regulated by Wnt/β-catenin signaling [22,23], our findings are consistent with this concept. Importantly, overall BV/TV was significantly higher in male mice compared to their female counterparts in both control and HET cKO genotypes.

We did not observe a significant difference in trabecular or cortical bone mineral density (material density by microCT) in these mice at 18–24 weeks of age compared to controls. We interpret this as indicating that the bone that is being made has the same material density in HET cKO mice versus controls, but the reduction in BV/TV indicates there is less bone present. The decrease in % ash content suggests that there is overall modestly reduced mineral in the combined cortical and trabecular compartments, which is likely due to reductions in the trabecular compartments.

Analysis of the biomechanical properties by 3-point bending of control and HET cKO mice showed no significant differences in male or female mouse femurs and their controls. The control female group had a significantly higher Young's Modulus compared to male control mice, which was not evident in the HET cKO group. Perhaps this relates to the greater decrease in BV/TV in female versus male HET cKO mice. The fact that the biomechanical properties were not different between male versus female HET cKO is consistent with both the cortical microCT data and the load:strain curve data, which also showed no differences between the genders. The deletion of a single allele of β–catenin in osteocytes mainly appears to affect trabecular bone at 18–24 weeks of age. It will be interesting to determine if older aged mice (up to 2 years of age) will eventually display cortical effects or if the changes will remain restricted to trabecular bone.

Our findings of gender differences related to β–catenin signaling has been observed in previous studies involving other components associated with the pathway, albeit not always discussed in detail. Yao *et al* [34] demonstrated that systemic overexpression of sFRP1, a negative regulator of the Wnt/β–catenin signaling pathway, resulted in an osteopenic skeleton in which distal femur BV/TV was decreased by 22% in females and 51% in males and midshaft cortical thickness was 13% lower in females and 21% lower in male mice. They also reported increased bone resorption in male mice, which appears to be a common finding in terms of the consequences of altered β–catenin signaling in bone that has been reported by others [22,23,35]. Data from the *Sost* null mouse [36] demonstrated a more pronounced BMD increase in the female mice compared to male mice, but was not discussed, most likely because the data was not specifically analyzed for gender differences. In a loading study performed with male and female *Lrp5* null mice, Sawakami *et al* [8] noted greater suppression of load-induced bone formation in female *Lrp5* null mice compared to males. Saxon *et al* also reported gender related differences in load and disuse studies of *Lrp5* null and *LRP5* high bone mass ($LRP5^{G171V}$) mice expressing human *LRP5* transgene containing the G171V activating mutation. The female $LRP5^{G171V}$ mice were more responsive to lower magnitudes of loads and had less bone loss in response to disuse compared to males [15]. Those authors also puzzled over a possible explanation for their observed gender differences, but speculated that a possible explanation could be the higher *Lrp5* mRNA expression level compared to controls [21]. Javaheri *et al*. reported gender related differences in proliferation and apoptosis in primary osteoblast-like cells isolated from *Lrp5* null and $LRP5^{G171V}$ mice compared to cells from wildtype littermates with cells

isolated from female *Lrp5*$^{-/-}$ and *LRP5*^{G171V} mice being more affected by LRP5-β-catenin signaling [37]. Interestingly, the bone biomechanical properties of female and male *LRP5*^{G171V} mice did not display gender differences in the study by Akhter *et al* [5], which further supports the complex nature of gender influences on β-catenin signaling and the need for more study. The mechanism underlying this gender difference and the greater sensitivity of the female skeleton to osteocyte β–catenin haploinsufficiency is not clear. The estrogen receptor-α has been shown to be important in β–catenin signaling in osteoblasts [11], while estrogen receptor-β appears to regulate sclerostin production [38]. It is reasonable to speculate that sex hormone differences could underlie this gender difference, but until studies with gonadectomy are performed in HET cKO mice, the exact mechanism remains unknown.

The Wnt/β–catenin signaling pathway is activated in response to mechanical loading [9,10,39]. We found that deletion of a single allele of β–catenin in osteocytes has a profound effect on the anabolic loading response. Ulnae for each group were loaded at a global load of ~2500 με. Surprisingly the new bone formation observed in response to *in vivo* mechanical loading in control mice was essentially absent in the HET cKO mice ulnae. This was demonstrated by both dynamic histomorphometry of double labeling and by microCT cortical bone thickness quantitation. These data support the concept that there is a critical level of β-catenin in osteocytes that is needed to develop a normal skeleton, adequately contributed by one allele of β-catenin, but the ability to mount a bone formation response to anabolic mechanical loading requires a higher level of β-catenin expression that requires both alleles.

Our findings suggest an intriguing, new paradigm for contextualizing bone mass regulation by the Wnt/β-catenin signaling pathway. Namely, that there is a critical stoichiometry for all of the key proteins comprising the Wnt/β-catenin signaling pathway that is required for the proper accrual and maintenance of a normal skeleton. The various mouse and human bone phenotypes that result from deletions or mutations of components of the Wnt/β-catenin pathway suggest functional redundancy of its' components [40]. As such it is not clear why deletions or mutations in any of these components produce a bone phenotype. This suggests to us that the stoichiometry of these various components must be critical. For example, the *LRP5* G171V or HBM transgenic mouse model expresses the human transgene against the background of two normal mouse alleles producing a high bone mass phenotype, whereas overexpression of the normal *LRP5* transgene only results in a modest increase in bone mass [21]. Deletion of the *Sost* gene produces a high bone mass phenotype [36], but in a background in which the expression of other Wnt pathway inhibitors such as *Dkk1* are normal. Similarly the *sFRP1* knockout mouse [20] has an increased bone mass phenotype even though presumably both Sost and Dkk1 expression are normal. *Lrp5* homozygous knockout mice have low bone mass [19], while *Lrp6* homozygous knockout mice die at birth and have multiple patterning defects [41], although studies in *Lrp5/Lrp6* mutant mice indicate that some amount of adult bone mass is also contributed by *Lrp6* [42]. *Lrp4* deficient mice have a low bone mass phenotype [43], yet both *Lrp5* and *Lrp6* are still present and normal. All of these models suggest that there is a critical, yet unknown, balance between each component of the pathway, and that this nominal equilibrium of all components is

needed for normal bone growth/mass and accrual. An additional level of complexity that is not understood is the differential expression at specific stages of development or response of individual components of this pathway to stimuli, or relative expression in specific cell types.

Another important consideration is the restricted role of the Wnt/β-catenin signaling pathway in osteocytes. The osteocyte is considered to be a terminally differentiated cell of the osteoblast lineage (For review see Dallas *et al*., 2013 [44]). It resides within the mineralized matrix and lacks the ability to divide when contained in that environment. Hence the normal proliferative and differentiation associated functions of the pathway are not operative in the osteocyte. Proliferation would appear to be a fatal event for the osteocyte in its lacunae given the space confinement. Therefore, at least two important functions of β-catenin signaling are abrogated in the case of the osteocyte. It appears that the pathway in osteocytes is used predominantly as an anti-apoptosis protective mechanism [45] and in proper response to loading, functions that are observed in many other cells/tissues and tumors [18,46–54].

In summary, we have demonstrated that mice with a heterozygous deletion of β–catenin in osteocytes lose the ability to form new bone in response to *in vivo* mechanical loading. The effects of osteocyte β–catenin haploinsufficiency are more severe in the female skeleton. These findings suggest that there is a threshold level of β–catenin in osteocytes that is required for new bone formation in response to *in vivo* mechanical loading that is different than the level required to form the skeleton and that regulation of the pathway is influenced gender. Our data indicate that a better appreciation of the subtle nuances of regulation of the Wnt/β-catenin signaling pathway at the level of the stoichiometry and balance of its various components is required. Secondly, a better understanding of the potential mitigating influences of gender is needed as new bone anabolic pharmaceutical agents are being developed that target components of this pathway.

Supplementary Material

Refer to Web version on PubMed Central for supplementary material.

Acknowledgments

We thank Ms. Anita Xie her expert technical assistance. This work was supported by NIH/NIAMS grants RO1 AR053949 (MLJ) and PO1 AR046798 (LFB). Author Roles: BJ: performed majority of experimental work presented, including *in vivo* forearm loading, microCT, histomorphometry and biomechanical testing, primary writing of manuscript. AS: performed biomechanical testing and analysis, writing of manuscript. NL: collation and analysis of data, performed the histology to determine TRAP positive osteoclasts, and writing of manuscript. MD: performed *in vivo* forearm loading, microCT and biomechanical testing. HZ: performed animal breeding, injections for double labeling, collection of bones for analysis. YL: performed statistical analysis of data. LFB: concept, experimental design and writing of manuscript. MLJ: concept, experimental design and overall supervision of project and writing of manuscript. All authors have reviewed and accept the data analysis in the manuscript.

References

1. Gong Y, Slee RB, Fukai N, Rawadi G, Roman-Roman S, Reginato AM, Wang H, Cundy T, Glorieux FH, Lev D, Zacharin M, Oexle K, Marcelino J, Suwairi W, Heeger S, Sabatakos G, Apte S, Adkins WN, Allgrove J, Arsian-Kirchner M, Batch JA, Beighton P, Black GCM, Boles RG,

Boon LM, Borrone C, Brunner HG, Carle GF, Dallapiccola B, De Paepa A, Floege B, Halfide ML, Hall B, Hennekam RC, Hirose T, Jans A, Juppner H, Kim CA, Keppler-Noreuil K, Kohlschuetter A, LaCombe D, Lambert M, Lemyre E, Letteboer T, Peltonen L, Ramesar RS, Romanengo M, Somer H, Steichen-Gersdorf E, Steinmann B, Sullivan B, Superta-Furga A, Swoboda W, van den Boogaard M-J, Van Hul W, Vikkula M, Votruba M, Zabel B, Garcia T, Baron R, Olsen BR, Warman ML. LDL Receptor-Related Protein 5 (LRP5) Affects Bone Accrual and Eye Development. Cell. 2001; 107:513–523. [PubMed: 11719191]

2. Little RD, Carulli JP, Del Mastro RG, Dupuis J, Osborne M, Folz C, Manning SP, Swain PM, Zhao SC, Eustace B, Lappe MM, Spitzer L, Zweier S, Braunschweiger K, Benchekroun Y, Hu X, Adair R, Chee L, FitzGerald MG, Tulig C, Caruso A, Tzellas N, Bawa A, Franklin B, McGuire S, Nogues X, Gong G, Allen KM, Anisowicz A, Morales AJ, Lomedico PT, Recker SM, Van Eerdewegh P, Recker RR, Johnson ML. A mutation in the LDL receptor-related protein 5 gene results in the autosomal dominant high-bone-mass trait. Am J Hum Genet. 2002; 70(1):11–9. [PubMed: 11741193]
3. Boyden LM, Mao J, Belsky J, Mitzner L, Farhi A, Mitnick MA, Wu D, Insogna K, Lifton RP. High Bone Density Due to a Mutation in LDL-Receptor-Related Protein 5. N Engl J Med. 2002; 346:1513–1521. [PubMed: 12015390]
4. Johnson ML, Picconi JL, Recker RR. The Gene for High Bone Mass. The Endocrinologist. 2002; 12:445–453.
5. Akhter MP, Wells DJ, Short SJ, Cullen DM, Johnson ML, Haynatzki GR, Babij P, Allen KM, Yaworsky PJ, Bex F, Recker RR. Bone biomechanical properties in LRP5 mutant mice. Bone. 2004; 35(1):162–9. [PubMed: 15207752]
6. Johnson ML. The High Bone Mass Family - The Role of Wnt/LRP5 Signaling in the Regulation of Bone Mass. J Mus Neuron Interact. 2004; 4(2):135–138.
7. Hens JR, Wilson KM, Dann P, Chen X, Horowitz MC, Wysolmerski JJ. TOPGAL Mice Show that the Canonical Wnt Signaling Pathway is Active during Bone Development and Growth and is Activated by Mechanical Loading In Vitro. J Bone Miner Res. 2005; 20:1103–1113. [PubMed: 15940363]
8. Sawakami K, Robling AG, Ai M, Pitner ND, Liu D, Warden SJ, Li J, Maye P, Rowe DW, Duncan RL, Warman ML, Turner CH. The Wnt Co-Receptor Lrp5 is Essential for Skeletal Mechanotransduction, but Not for the Anabolic Bone Response to Parathyroid Hormone Treatment. J Biol Chem. 2006; 281:23698–23711. [PubMed: 16790443]
9. Lau K-HW, Kapur S, Kesavan C, Baylink DJ. Up-Regulation of the Wnt, Estrogen Receptor, Insulin-like Growth Factor-I, and Bone Morphogenetic Protein Pathways in C57BL/6J Osteoblasts as Opposed to C3H/HeJ Osteoblasts in Part Contributes to the Differential Anabolic Response to Fluid Shear. J Biol Chem. 2006; 281:9576–9588. [PubMed: 16461770]
10. Robinson JA, Chatterjee-Kishore M, Yaworsky P, Cullen DM, Zhao W, Li C, Kharode YP, Sauter L, Babij P, Brown EL, Hill AA, Akhter MP, Johnson ML, Recker RR, Komm BS, Bex FJ. Wnt/b-Catenin Signaling is a Normal Physiological Response to Mechanical Loading in Bone. J Biol Chem. 2006; 281:31720–31728. [PubMed: 16908522]
11. Armstrong VJ, Muzylak M, Sunters A, Zaman G, Saxon LK, Price JS, Lanyon LE. Wnt/b-Catenin signaling is a Component of Osteoblastic Bone Cell Early Responses to Load-bearing and Requires Estrogen Receptor a. J Biol Chem. 2007; 282:20715–20727. [PubMed: 17491024]
12. Armstrong VJ, Muzylak M, Sunters A, Zaman G, Saxon LK, Price JS, Lanyon LE. Estrogen Receptor a is Required for Strain-Related b-Catenin Signaling in Osteoblasts. J Bone Min Res. 2007; 22(suppl 1):S95. abstr S064.
13. Kamel MA, Picconi JL, Lara-Castillo N, Johnson ML. Activation of beta-catenin signaling in MLO-Y4 osteocytic cells versus 2T3 osteoblastic cells by fluid flow shear stress and PGE(2): Implications for the study of mechanosensation in bone. Bone. 2010; 47(5):872–881. [PubMed: 20713195]
14. Santos A, Bakker AD, Zandieh-Doulabi B, de Blieck-Hogervorst JM, Klein-Nulend J. Early activation of the beta-catenin pathway in osteocytes is mediated by nitric oxide, phosphatidyl inositol-3 kinase/Akt, and focal adhesion kinase. Biochem Biophys Res Commun. 2010; 391(1): 364–9. [PubMed: 19913504]

15. Saxon LK, Jackson BF, Sugiyama T, Lanyon LE, Price JS. Analysis of multiple bone responses to graded strains above functional levels, and to disuse, in mice in vivo show that the human Lrp5 G171V High Bone Mass mutation increases the osteogenic response to loading but that lack of Lrp5 activity reduces it. Bone. 2011; 49(2):184–193. [PubMed: 21419885]
16. Bonewald LF, Johnson ML. Osteocytes, mechanosensing and Wnt signaling. Bone. 2008; 42:606–615. [PubMed: 18280232]
17. Sunters A, Armstrong VJ, Zaman G, Kypta RM, Kawano Y, Lanyon LE, Price JS. Mechano-transduction in Osteoblastic Cells Involves Strain-regulated Estrogen Receptor a-mediated Control of Insulin-like Growth Factor (IGF) I Receptor Sensitivity to Ambient IGF, Leading to Phosphatidylinositol 3-Kinase/AKT-dependent Wnt/LRP5 Receptor-independent Activation of beta-Catenin Signaling. Journal of Biological Chemistry. 2010; 285(12):8743–8758. [PubMed: 20042609]
18. Reya T, Clevers H. Wnt Signalling in Stem Cells and Cancer. Nature. 2005; 434:843–850. [PubMed: 15829953]
19. Kato M, Patel MS, Levasseur R, Lobov I, Chang BH-J, Glass DA, Hartmann C, Li L, Hwang TH, Brayton CF, Lang RA, Karsenty G, Chan L. Cbfa 1-Independent Decrease in Osteoblast Proliferation, Osteopenia, and Persistent Embryonic Eye Vascularization in Mice Deficient in Lrp5, a Wnt Coreceptor. J Cell Biol. 2002; 157:303–314. [PubMed: 11956231]
20. Bodine PVN, Zhao W, Kharode YP, Bex FJ, Lambert A-J, Goad MB, Gaur T, Stein GS, Lian JB, Komm BS. The Wnt Antagonist Secreted Frizzled-Related Protein-1 is a Negative Regulator of Trabecular Bone Formation in Adult Mice. Mole Endocrin. 2004; 18:1222–1237.
21. Babij P, Zhao W, Small C, Kharode Y, Yaworsky P, Bouxsein M, Reddy P, Bodine P, Robinson J, Bhat B, Marzolf J, Moran R, Bex F. High Bone Mass in Mice Expressing a Mutant LRP5 Gene. J Bone Miner Res. 2003; 18:960–974. [PubMed: 12817748]
22. Glass DA, Bialek P, Ahn JD, Starbuck M, Patel MS, Clevers H, Taketo MM, Long F, McMahon AP, Lang RA, Karsenty G. Canonical Wnt Signaling in Differentiated Osteoblasts Controls Osteoclast Differentiation. Develop Cell. 2005; 8:751–764.
23. Holmen SL, Zylstra CR, Mukherjee A, Sigler RE, Faugere M-C, Bouxsein ML, Deng L, Clemens TL, Williams BO. Essential Role of *b*-Catenin in Postnatal Bone Acquisition. J Biol Chem. 2005; 280:21162–21168. [PubMed: 15802266]
24. Kramer I, Halleux C, Keller H, Pegurri M, Gooi JH, Weber PB, Feng JQ, Bonewald LF, Kneissel M. Osteocyte Wnt/b-Catenin Signaling Is Required for Normal Bone Homeostasis. Mol. Cell. Biol. 2010; 30:3071–3085. [PubMed: 20404086]
25. Nakashima T, Hayashi M, Fukunaga T, Kurata K, Oh-hora M, Feng JQ, Bonewald LF, Kodama T, Wutz A, Wagner EF, Penninger JM, Takayanagi H. Evidence for osteocyte regulation of bone homeostasis through RANKL expression. Nat Med. 2011; 17(10):1231–1234. [PubMed: 21909105]
26. Wijenayaka AR, Kogawa M, Lim HP, Bonewald LF, Findlay DM, Atkins GJ. Sclerostin Stimulates Osteocyte Support of Osteoclast Activity by a RANKL-Dependent Pathway. PLoS ONE. 2011; 6(10):e25900. [PubMed: 21991382]
27. Xiong J, Onal M, Jilka RL, Weinstein RS, Manolagas SC, O'Brien CA. Matrix-embedded cells control osteoclast formation. Nat Med. 2011; 17(10):1235–1241. [PubMed: 21909103]
28. Lu Y, Xie Y, Zhang S, Dusevich V, Bonewald LF, Feng JQ. DMP1-targeted Cre expression in odontoblasts and osteocytes. J Dent Res. 2007; 86(4):320–5. [PubMed: 17384025]
29. Dempster DW, Compston JE, Drezner MK, Glorieux FH, Kanis JA, Malluche H, Meunier PJ, Ott SM, Recker RR, Parfitt AM. Standardized nomenclature, symbols, and units for bone histomorphometry: A 2012 update of the report of the ASBMR Histomorphometry Nomenclature Committee. Journal of Bone and Mineral Research. 2013; 28(1):2–17. [PubMed: 23197339]
30. Bouxsein ML, Boyd SK, Christiansen BA, Guldberg RE, Jepsen KJ, Müller R. Guidelines for assessment of bone microstructure in rodents using micro-computed tomography. Journal of Bone and Mineral Research. 2010; 25(7):1468–1486. [PubMed: 20533309]
31. Korecki C, Zinser G, Liu X, Siedler J, Welsh J, Niebur G. Effect of the Vitamin D Receptor on Bone Geometry and Strength During Gestation and Lactation in Mice. Calcified Tissue International. 2009; 85(5):405–411. [PubMed: 19763375]

32. Doube M, Kłosowski MM, Arganda-Carreras I, Cordelières FP, Dougherty RP, Jackson JS, Schmid B, Hutchinson JR, Shefelbine SJ. BoneJ: Free and extensible bone image analysis in ImageJ. Bone. 2010; 47(6):1076–1079. [PubMed: 20817052]
33. Schneider CA, Rasband WS, Eliceri KW. NIH IMage to ImageJ: 25 Years of Image Analysis. Nature Methods. 2012; 9:671–675. [PubMed: 22930834]
34. Yao W, Cheng Z, Shahnazari M, Dai W, Johnson ML, Lane NE. Overexpression of secreted frizzled-related protein 1 inhibits bone formation and attenuates parathyroid hormone bone anabolic effects. Journal of Bone and Mineral Research. 2010; 25(2):190–199. [PubMed: 19594295]
35. Diarra D, Stolina M, Polzer K, Zwerina J, Ominsky MS, Dwyer D, Korb A, Smolen J, Hoffmann M, Scheinecker C, van der Heide D, Landewe R, Lacey D, Richards WG, Schett G. Dickkopf-1 is a Master Regulator of Joint Remodeling. Nature Med. 2007; 13:156–163. [PubMed: 17237793]
36. Li X, Ominsky MS, Niu Q-T, Sun N, Daugherty B, D'Agostin D, Kurahara C, Gao Y, Cao J, Gong J, Asuncion F, Barrero M, Warmington K, Dwyer D, Stolina M, Morony S, Sarosi I, Kostenuik PJ, Lacey DL, Simonet WS, Ke HZ, Paszty C. Targeted Deletion of the Sclerostin Gene in Mice Results in Increased Bone Formation and Bone Strength. Journal of Bone and Mineral Research. 2008; 23(6):860–869. [PubMed: 18269310]
37. Javaheri B, Sunters A, Zaman G, Suswillo RF, Saxon LK, Lanyon LE, Price JS. Lrp5 is not required for the proliferative response of osteoblasts to strain but regulates proliferation and apoptosis in a cell autonomous manner. PLoS One. 2012; 7(5):e35726. [PubMed: 22567110]
38. Galea GL, Meakin LB, Sugiyama T, Zebda N, Sunters A, Taipaleenmaki H, Stein GS, van Wijnen AJ, Lanyon LE, Price JS. Estrogen Receptor α Mediates Proliferation of Osteoblastic Cells Stimulated by Estrogen and Mechanical Strain, but Their Acute Down-regulation of the Wnt Antagonist Sost Is Mediated by Estrogen Receptor β. Journal of Biological Chemistry. 2013; 288(13):9035–9048. [PubMed: 23362266]
39. Xing W, Baylink D, Kesavan C, Hu Y, Kapoor S, Chadwick RB, Mohan S. Global gene expression analysis in the bones reveals involvement of several novel genes and pathways in mediating an anabolic response of mechanical loading in mice. Journal of Cellular Biochemistry. 2005; 96(5):1049–1060. [PubMed: 16149068]
40. Johnson ML. LRP5 and bone mass regulation: Where are we now? BoneKEy Rep. 2012; 1:1–6. [PubMed: 23951413]
41. Pinson KI, Brennan J, Monkley S, Avery BJ, Skarnes WC. An LDL-Receptor-Related Protein Mediates Wnt Signalling in Mice. Nature. 2000; 407:535–538. [PubMed: 11029008]
42. Holmen SL, Giambernardi TA, Zylstra CR, Buckner-Berghuis BD, Resau JH, Hess JF, Glatt V, Bouxsein ML, Ai M, Warman ML, Williams BO. Decreased BMD and Limb Deformities in Mice Carrying Mutations in Both Lrp5 and Lrp6. J Bone Miner Res. 2004; 19:2033–2040. [PubMed: 15537447]
43. Choi HY, Dieckmann M, Herz J, Niemeier A. Lrp4, a Novel Receptor for Dickkopf 1 and Sclerostin, Is Expressed by Osteoblasts and Regulates Bone Growth and Turnover *In Vivo*. PLoS One. 2009; 4(11):e7930. [PubMed: 19936252]
44. Dallas, SL.; Prideaux, M.; Bonewald, LF. The Osteocyte: An Endocrine Cell and More. 2013. Endocrine Reviews *ePub* ahead of print
45. Kitase Y, Barragan L, Jiang JX, Johnson ML, Bonewald LF. Mechanical induction of PGE(2) in osteocytes blocks glucocorticoid induced apoptosis through both the beta-catenin and PKA pathways. J Bone Miner Res. 2010; 25(12):2657–2668. [PubMed: 20578217]
46. Sen B, Styner M, Xie Z, Case N, Rubin CT, Rubin J. Mechanical loading regulates NFATc1 and beta-catenin signaling through a GSK3beta control node. J Biol Chem. 2009; 284(50):34607–17. [PubMed: 19840939]
47. Case N, Ma M, Sen B, Xie Z, Gross TS, Rubin J. Beta-catenin levels influence rapid mechanical responses in osteoblasts. J Biol Chem. 2008; 283(43):29196–205. [PubMed: 18723514]
48. Srivastava T, McCarthy ET, Sharma R, Cudmore PA, Sharma M, Johnson ML, Bonewald LF. Prostaglandin E2 is crucial in the response of podocytes to fluid flow shear stress. J Cell Commun Signal. 2010; 4(2):79–90. [PubMed: 20531983]

49. Monga SPS. Role of Wnt/β-catenin signaling in liver metabolism and cancer. The international journal of biochemistry & cell biology. 2011; 43(7):1021–1029. [PubMed: 19747566]
50. Nathke I. Cytoskeleton out of the cupboard: colon cancer and cytoskeletal changes induced by loss of APC. Nat Rev Cancer. 2006; 6(12):967–974. [PubMed: 17093505]
51. Polakis P. Wnt Signaling and Cancer. Genes Develop. 2000; 14:1837–1851. [PubMed: 10921899]
52. Logan CY, Nusse R. The Wnt Signaling Pathway in Development and Disease. Annual Rev. Cell Dev. Biol. 2004; 20:781–810. [PubMed: 15473860]
53. Nusse R. Wnt Signaling in Disease and Development. Cell Research. 2005; 15:28–32. [PubMed: 15686623]
54. Bodine PVN, Komm BS. Wnt Signaling and Osteoblastogenesis. 2006; 7:33–39. Reviews in Endocrine & Metabolic Disorders.

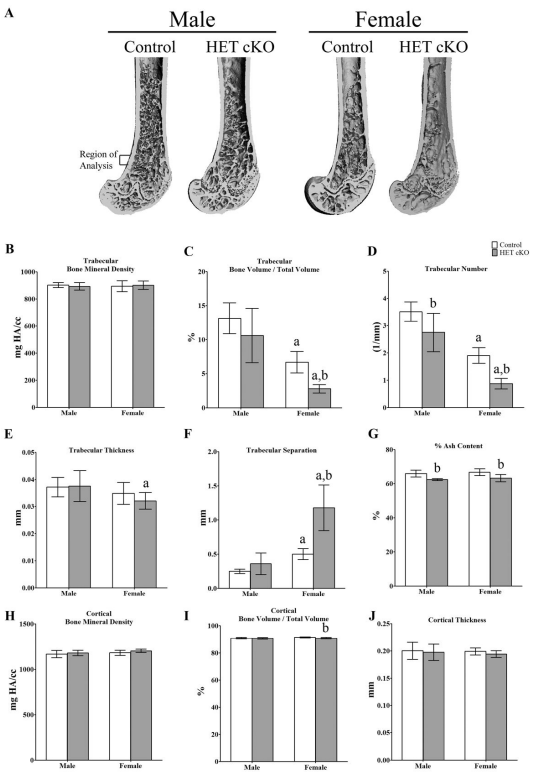

Figure 1.

Bone phenotype of control and HET cKO femurs. A) Representative 3D μCT images of femoral trabecular bone. Ex-vivo high-resolution analyses of distal femurs to determine B) trabecular Bone Mineral Density (BMD), C) trabecular bone volume / total volume (BV/TV) D) trabecular number, E) trabecular thickness, F) trabecular separation G) percentage ash content. H) Cortical BMD, I) cortical BV / TV and J) cortical thickness in control (white bars) and HET cKO mice (gray bars). (B–G) Bar graphs represent means plus SD. Group size n=7 for male and female controls and male HET cKO mice; n=9 for HET cKO mice. Statistical comparisons; a: $p<0.05$ between male and female of same genotype b: $p<0.05$ comparing control to HET cKO.

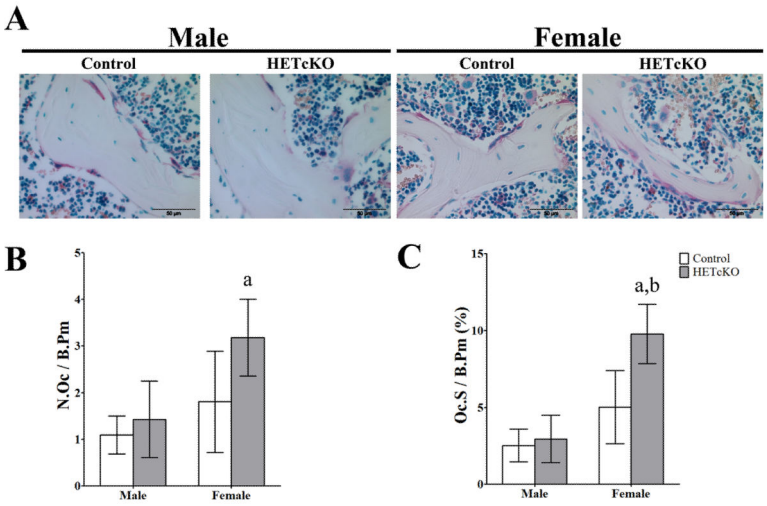

Figure 2.

Female β–catenin heterozygous deleted mice showed increase osteoclast activity compared to their controls. A) Shows representative images of fixed sections from femurs. Images were taken using 40X objective bar = 50μm. B) Histomorphometric quantitation of osteoclast number per bone perimeter. C) Histomorphometric quantitation of osteoclast surface per bone perimeter. Group size n=3 for controls, male and female, and male HET cKO mice. Statistical comparison a: $p<0.05$ between male and female of same genotype b: $p<0.05$ comparing control to HET cKO.

A

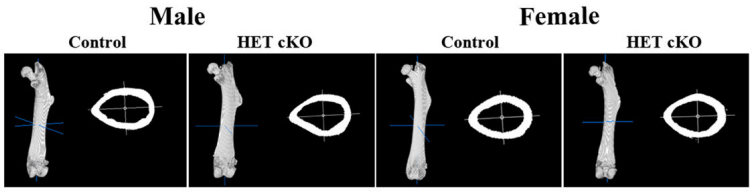

B

	Male		Female	
	Control	HET cKO	Control	HET cKO
Stiffness (N/mm)	128.88 ± 22.37	115.88 ± 9.96	115.28 ± 10.27	114.22 ± 22.78
Ultimate Force (N)	16.411 ± 4.78	16.16 ± 4.29	15.62 ± 1.00	15.15 ± 1.68
Young's Modulus (GPa)	5.69 ± 0.99	6.532 ± 2.34	8.74 ± 1.31[a]	9.13 ±2.08[a]

Figure 3.

Biomechanical properties of control femurs as compared to HET cKO. A) Representative 3D images of entire femur and cortical cross section using the BoneJ plug-in (ImageJ). B) Table listing the biomechanical parameters: Stiffness, Ultimate Force and Young's Modulus. Group size n=8 for male controls and HET cKO; n=6 for and female controls; n=10 for female HET cKO mice. Statistical comparisons; a: $p<0.05$ between male and female of same genotype.

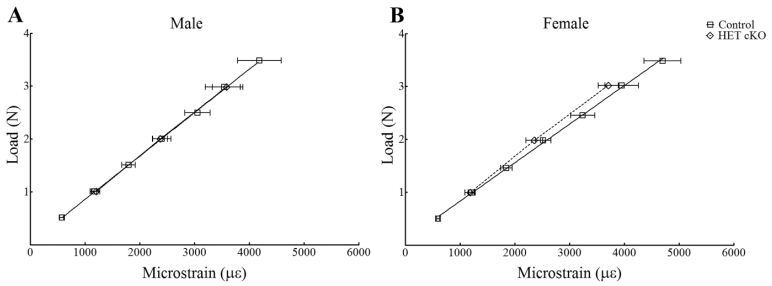

Figure 4.

Strain gage analysis of male (Panel A) and female (Panel B) control and HET cKO ulnae to determine the load:strain relationship. Group size n=4 for female HET cKO, n=4 for males HET cKO, female controls n=3 and male controls n=3.

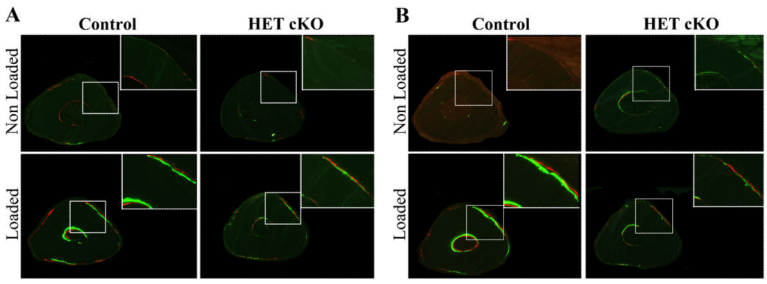

Figure 5.

β-catenin heterozygous mice have decreased response to loading. Representative images of double fluorochrome labeling using calcein and alizarin red of loaded and non-loaded ulnae 3 mm distal to the midshaft region. Panel A: Male control and HET cKO mice. Panel B: Female control and HET cKO mice. Right top corner shows a magnification of similar regions to better visualize double labeling. Sections were viewed under fluorescent light to observe mineral deposition due to loading. Control females and males showed clear double labeling after loading; this response was absent in β-catenin heterozygous mice.

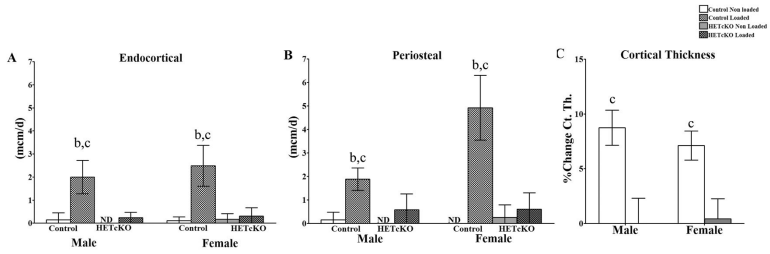

Figure 6.

Histomorphometric analysis of mineral apposition rates on periosteal and endosteal surfaces of loaded and non-loaded ulnae. A) endocortical and B) periosteal surface analysis. Group size was n=5 for males and n=4 for females. C) Representative percent change in cortical thickness comparing loaded to non-loaded ulnae using μCT analysis. Statistical comparisons; b: $p<0.05$ comparing control to HET cKO; c: $p<0.05$ comparing non-loaded versus loaded.

Table 1

β-catenin heterozygous knockout mice do not respond to loading. Data represent mean ± SD for bone formation rate/bone surface (BFR/BS), bone formation rate/bone volume (BFR/BV), bone formation rate/total volume (BRF/TV), single labeled surface per bone perimeter (sL.S/B.Pm), and double labeled surface per bone perimeter (dL.S/B.Pm) in the endocortical and periosteal region. Group size n=5 for male controls and HET cKO, n=4 for female controls and HET cKO. a = statistically significant different comparing male to female; b = statistically significantly different comparing control versus HET cKO; and c = statistically significant different between non loaded and loaded ulna. Statistical significance was determined using a two independent sample t-test (control and HET cKO) and matched paired t-test for left and right (load, non-loaded).

		Male				Female			
		Control		HET cKO		Control		HET cKO	
		Non-Loaded	Loaded	Non-Loaded	Loaded	Non-Loaded	Loaded	Non-Loaded	Loaded
Endocortical	BFR/BS ($mcm^3/mcm^2/d$)	0.01 ± 0.01	1.43 ± 0.19 ^{b,c}	ND	0.03 ± 0.02	0.01 ± 0.01	1.71 ± 0.36^{b,c}	0.03 ± 0.02	0.05 ± 0.05
	BFR/BV (%/y)	0.01 ± 0.01	0.35 ± 0.06^{b,c}	ND	0.01 ± 0.01	ND	0.63 ± 0.14^{b,c}	0.01 ± 0.01	0.01 ± 0.01
	BFR/TV (%/y)	ND	0.32 ± 0.05 ^{b,c}	ND	0.01 ± 0.1	ND	0.54 ± 0.11^{b,c}	0.01 ± 0.01	0.01 ± 0.01
	Ec.sL.S/B.Pm (%)	14.0 ± 10.3	51.40 ± 13.50	7.48 ± 6.83	8.80 ± 8.30	12.09 ± 4.29	47.01 ± 4.96	7.60 ± 1.30	5.97 ± 0.54
	Ec.dL.S/B.Pm (%)	1.80 ± 4.10	75.50 ± 35.70	ND	4.30 ± 4.90	1.12 ± 1.94	70.31 ± 26.45	3.72 ± 5.24	6.46 ± 10.19
Periosteal	BFR/BS ($mcm^3/mcm^2/d$)	0.01 ± 0.01	0.49 ± 0.13^{a,b,c}	ND	0.07 ± 0.06	ND	1.57 ± 0.16^{b,c}	0.02 ± 0.02	0.08 ± 0.05
	BFR/BV (%/y)	0.01 ± 0.01	0.44 ± 0.13^{a,b,c}	ND	0.07 ± 0.05	ND	1.55 ± 0.15^{b,c}	0.02 ± 0.02	0.07 ± 0.04
	BFR/TV (%/y)	0.01 ± 0.01	0.39 ± 0.11^{a,b,c}	ND	0.06 ± 0.05	ND	1.33 ± 0.14^{b,c}	0.01 ± 0.02	0.06 ± 0.04
	Ps.sL.S/B.Pm	5.44 ± 4.44	43.36 ± 9.75 ^{b,c}	1.78 ± 2.05	8.58 ± 3.19	4.46 ± 3.51	35.83 ± 5.15^{b,c}	0.70 ± 0.72	5.71 ± 5.14
	Ps.dL.S/B.Pm (%)	1.52 ± 3.41	25.09 ± 7.94^{b,c}	ND	3.35 ± 4.07	ND	33.33 ± 7.67^{b,c}	1.64 ± 3.27	5.21 ± 6.19